Published in final edited form as:
Arthroscopy. 2013 January ; 29(1): 122–132. doi:10.1016/j.arthro.2012.07.006.

Effects of Suture Choice on Biomechanics and Physeal Status After Bioenhanced Anterior Cruciate Ligament Repair in Skeletally Immature Patients: A Large-Animal Study

Patrick Vavken, M.D., M.Sc., **Benedikt Proffen, M.D.**, **Chris Peterson, B.S.**, **Braden C. Fleming, Ph.D.**, **Jason T. Machan, Ph.D.**, and **Martha M. Murray, M.D.**
Sports Medicine Research Laboratory, Department of Orthopedic Surgery, Children's Hospital Boston (P.V., B.P., C.P., M.M.M.), Harvard Medical School, Boston, Massachusetts; Departments of Orthopaedics (B.C.F., J.T.M.) and Surgery (J.T.M.), Warren Alpert Medical School, Brown University, Providence, Rhode Island; Department of Research, Biostatistics (J.T.M.), Rhode Island Hospital, Providence, Rhode Island, U.S.A.; and Orthopaedic Department (P.V.), University Hospital Basel, Basel, Switzerland

Abstract

Purpose—The objective of this study was to assess the effect of absorbable or nonabsorbable sutures in bioenhanced anterior cruciate ligament (ACL) repair in a skeletally immature pig model on suture tunnel and growth plate healing and biomechanical outcomes.

Methods—Sixteen female skeletally immature Yorkshire pigs were randomly allocated to receive unilateral, bioenhanced ACL repair with an absorbable (Vicryl) or nonabsorbable (Ethibond) suture augmented by an extracellular matrix-based scaffold (MIACH). After 15 weeks of healing, micro–computed tomography was used to measure residual tunnel diameters and growth plate status, and biomechanical outcomes were assessed.

Results—At 15 weeks postoperatively, there was a significant difference in tunnel diameter with significantly larger diameters in the nonabsorbable suture group (4.4 ± 0.3 mm; mean ± SD) than in the absorbable group (1.8 ± 0.5 mm; P <.001). The growth plate showed a significantly greater affected area in the nonabsorbable group (15.2 ± 3.4 mm^2) than in the absorbable group (2.7 ± 0.8 mm^2, P < .001). There was no significant difference in the linear stiffness of the repairs (29.0 ± 14.8 N/mm for absorbable v 43.3 ± 28.3 N/mm for nonabsorbable sutures, P = .531), but load to failure was higher in the nonabsorbable suture group (211 ± 121.5 N) than in the absorbable suture group (173 ± 101.4 N, P =.002). There was no difference between the 2 groups in anteroposterior laxity at 30° (P = .5117), 60° (P = .3150), and 90° (P = .4297) of knee flexion.

Conclusions—The use of absorbable sutures for ACL repair resulted in decreased physeal plate damage after 15 weeks of healing; however, use of nonabsorbable sutures resulted in 20% stronger repairs.

Clinical Relevance—Choice of suture type for ACL repair or repair of tibial avulsion fractures may depend on patient skeletal age and size, with absorbable sutures preferred in very young, small patients at higher risk with physeal damage and nonabsorbable sutures preferred in larger, prepubescent patients who may place higher loads on the repair.

Address correspondence to Patrick Vavken, M.D., M.Sc., Department of Orthopedic Surgery, Children's Hospital Boston, Harvard Medical School, 300 Longwood Avenue, Enders 260, Boston, MA 02115, U.S.A. patrick.vavken@childrens.harvard.edu.

The authors report that they have no conflicts of interest in the authorship and publication of this article.

Recent studies have introduced the groundwork for a new treatment option for midsubstance anterior cruciate ligament (ACL) ruptures: bioenhanced ACL repair.[1] To the many who have followed the evolution of ACL surgery with great interest, it is somewhat inconceivable that primary repair of the ACL could ever work, given the high rates of failures noted in the past.[2] However, we have previously noted that the mechanistic defect in intrinsic ACL repair is the premature loss of the provisional scaffold in the ACL wound site. In tissues outside the joint, like the medial collateral ligament, when the tissue is torn, a blood clot forms between the 2 ends of the tissue and serves as a bridge, or provisional scaffold, between the 2 torn ends. The surrounding cells are then stimulated to crawl into this scaffold and remodel it into a functional fibrovascular scar. However, the blood clot that works so efficiently for structures outside of the joint is prematurely dissolved in the intrasynovial environment of the human ACL.[3,4] We have documented that in vivo placement of a stable bridge between the 2 ends of the ACL will allow cells to migrate into the wound site and heal it in animal studies.[3–5] There are several required properties of this scaffold – not only does it need to be stable in the joint environment,[6] but it also needs to contain some sort of biologic stimulus.[7] Collagen is an excellent choice as the basis for this scaffold, as it confers enzymatic resistance to enzymes commonly found in post-traumatic synovial fluid[8] and it is also a physiologic activator of platelets.[9,10] The scaffold used in this study is collagen-based, but also contains several other extracellular matrix molecules that are critical to its function as a substitute provisional scaffold. When this scaffold is combined with the cells found in blood, it is capable of releasing multiple cytokines critical to wound healing,[9,10] and it stimulates the migration, proliferation, and collagen production of the local ACL fibroblasts.[11] This combination of extracellular matrix scaffold and blood has been shown to result in healing of the ACL with similar properties to those seen with ACL reconstruction in a large-animal model.[12]

The bioenhanced ACL repair procedure is a primary suture repair of the ACL augmented with a biologic stimulus. Blood is an excellent biologic stimulus as it contains platelets (a source of anabolic factors beneficial for wound healing[13]), red blood cells (a source of oxygen metabolites[14]), and extracellular matrix proteins such as fibronectin[13]) – all factors important in early wound healing. The bioenhanced repair technique involves placement of an extracellular matrix–based carrier into the ACL defect and then saturating the scaffold with autologous whole blood.[12] This biologic composite is secured into the ACL defect using a suture bridge to initially protect the healing ligament.[12]

We have previously done this successfully using a collagen-based scaffold that contains additional extra-cellular matrix proteins and combining this with autologous whole blood.[12] The composite is secured into the ACL defect using a suture bridge to initially protect the healing ligament.[15] In an earlier study, it was shown that this bioenhanced ACL repair technique produced equivalent biomechanical results to a bone–patellar tendon–bone ACL reconstruction in a large animal model,[12] including measures of yield load, failure load, and ACL linear stiffness. Skeletally immature patients might benefit particularly from such a procedure, because of their relatively high intrinsic healing potential.[16,17] This same surgical bioenhanced repair technique was used in this study.

The technique of bioenhanced ACL repair currently uses a transphyseal suture stent, which requires drilling a 4-mm hole across the distal femoral and proximal tibial physis. This technique thus potentially places these physes at risk for damage.[18] The use of a nonabsorbable suture for the bioenhanced ACL repair may result in a permanent structure across the physis, as opposed to an absorbable suture, which would be resorbed in a matter of weeks. Whether these 2 suture types would affect the physis differently is unknown, but it is of interest not only for this new ACL repair technique but also for transphyseal suture fixation of tibial spine fractures, which is currently practiced.

In addition to the question of the physeal reaction to different suture types, the selection of suture may affect the overall strength of the healing ACL. The stent provides initial biomechanical stability and mechanical protection during remodeling. Nonabsorbable sutures might be beneficial as they protect the repair for an extended period of time, but they might also cause stress shielding, which has a detrimental effect on tissue remodeling.[19,20] Absorbable sutures, in turn, may reduce stress shielding but also may break down too early and expose the repair tissue to excessive mechanical stress and/or release breakdown products such as glycolic acid (from polyglycolic acid) or lactic acid (from polylactic acid), which reduce tissue pH and inhibit cell growth.[21–24]

The objectives of this study were 2-fold. The primary objective was to assess, using micro–computed tomography (CT), the effect on suture tunnel and growth plate healing of bioenhanced ACL repair in a skeletally immature pig model using either absorbable (Vicryl; Ethicon, Somerville, NJ) or nonabsorbable sutures (Ethibond; Ethicon) for the suture stent. The secondary objective was to compare the biomechanical outcomes at 15 weeks using the same 2 types of sutures by evaluating the structural properties of the repair (ie, yield and failure displacements, yield and failure loads, linear stiffness) and the anteroposterior (AP) laxity of the knee joint. We hypothesized that absorbable sutures would lead to better tunnel and growth plate healing and better biomechanical outcomes.

Methods

Study Design

The study protocol was approved by the responsible Institutional Animal Care and Use Committee. The study was designed as an assessor-blinded, randomized, controlled, large animal trial. Based on an a priori sample size calculation, a total of 16 female skeletally immature Yorkshire pigs (11.6 ± 0.2 weeks of age, 30 ± 0.1 kg body weight [mean ± SD]) were used and randomly allocated (using a sequence of random numbers) to 2 groups: bioenhanced ACL repair with an absorbable (Vicryl, n = 8) or nonabsorbable (Ethibond, n = 8) suture stent. Details regarding the power analyses are provided later. A unilateral repair was performed in all animals and the contralateral knee was used as an intact control for normalization.

The animals were euthanized after 15 weeks of healing, as that time point is well beyond the nadir in strength that occurs between 6 and 9 weeks after repair and is in the time period at which tissue maturation and generation of biomechanical strength are increasing.[5,15]

Collagen Scaffold Production

The extracellular matrix scaffolds (MIACH, Children's Hospital Boston, Boston, MA) were manufactured in our laboratory as previously described.[7,25,26] Briefly, extracellular matrix slurry was produced by sterilely solubilizing bovine connective tissue using salt extraction followed by pepsin digestion. All steps in the manufacturing process were performed under sterile conditions and no terminal sterilization was performed. The collagen concentration of this slurry was adjusted to at least 10 mg/mL. The slurry was frozen and lyophilized in a cylindrical mold to create a collagen sponge of 30 mm in length and 22 mm in diameter. All sponges were stored at −80°C until implantation.

Surgical Procedure

The surgical technique and model used in this study have been shown to be an effective repair of a mid-substance ACL defect, producing results that are not different from ACL reconstruction.[12] Bioenhanced repair was performed as previously described using small tunnels that come into the joint at the center of the tibial and femoral ACL footprints.[12] Two

types of sutures were used for this experiment: Vicryl is an absorbable, polyglactin suture that completely dissolves in approximately 63 days.[27,28] According to the manufacturer its strength decreases by 25% per week after the first week of implantation in situ. Ethibond is a nonabsorbable, braided poly-(ethylene, terephthalate) suture and does not lose strength as long as it remains intact. A recent study showed that these 2 sutures have virtually identical biomechanical properties, with a maximum load to failure of 130 ± 9 N versus 134 ± 9 N and linear stiffness of 15 ± 1 versus 13 ± 2 for Vicryl and Ethibond.[29]

All animals underwent unilateral ACL transsection. Under general anesthesia, a medial arthrotomy was made and the fat-pad was partially resected to expose the ACL. The ACL was cut with a scalpel at the junction between the proximal and middle thirds of the ligament. All knees showed tibiofemoral subluxation to verify complete transection. The knee was irrigated with 500 mL of normal saline.

For the bioenhanced ACL repair, a Kessler suture using No. 1 Vicryl was placed in the tibial stump of the ACL to repair the transected ligament in all ACL transsected knees.[7] Tunnels in the femur (4.5 mm) and tibia (2.4 mm) were created in the standard positions for ACL reconstruction, with the tibial tunnel exiting in the center of the tibial attachment and the femoral tunnel placed in the center of the femoral ACL attachment site. An EndoButton (Smith & Nephew Endoscopy, Andover, MA) armed with 3 sutures was pulled through the femoral tunnel and engaged on the femoral cortex. Two of these sutures were used to create the suture stent and were either Vicryl or Ethibond, depending on the group allocation of the animal. The stent was threaded through the scaffold with a straight needle, passed through the tibial tunnel, and tied over a button with the knee in full extension. At this point, 5 mL of autologous blood was drawn and the MIACH scaffold was saturated in situ with 3 mL of blood. The average platelet counts for the 2 groups were 325.000 ± 69.000/μL and 309.000 ± 128.000/μL ($P = .758$). The remaining third suture from the femoral tunnel/EndoButton was made of Vicryl and tied to the suture in the tibial ACL stump to reduce the tibial stump of the ACL into its physiologic position. Three knots were tied in each suture. The knee was left untouched for 10 minutes to allow clotting before the incisions were closed in layers.

After 15 weeks of healing, all animals were euthanized and both hindlimbs were harvested by hip disarticulation. All limbs were frozen and stored at −20°C.

Physical Examination

All animals underwent a physical examination under anesthesia preoperatively and before euthanasia, and values for knee flexion and extension and thigh circumference were recorded.

Biomechanical Testing

Biomechanical testing included AP knee laxity and tensile strength testing. Tensile strength testing was done at time zero and at 15 weeks to assess the strength of the graft stent and the repair tissue. AP knee laxity testing was done at 15 weeks only since an earlier publication already showed that primary repair restores AP laxity compared with normal at time zero.[30] The knees were thawed at room temperature and all soft tissue surrounding the tibia and femur were removed, leaving the capsule intact.[7,25,26] All specimens were potted in Schedule 40 PVC pipe tubes using urethane potting compound (Smooth On, Easton, PA), oriented such that the long axes of the bone and tubes were parallel. All testing was done using an MTS 810 servohydraulic load frame (MTS Systems, Eden Prairie, MN). All mechanical testing evaluators were blinded as to treatment group during the testing process.

AP knee testing was performed with the knee flexion angle set at 30°, 60°, and 90°, respectively, by applying fully reversed, sinusoidal AP-directed shear loads of ±40 N at

0.0833 (one-twelfth) Hz for 12 cycles in each position as previously described.[7,25,26] During the AP laxity tests, axial rotation was locked in the neutral position, whereas the varus-valgus angulation and the coronal plane translations were left unconstrained. Data for load and displacement were collected at 20 Hz.

The structural properties of the ligament or graft constructs were then determined using a tensile test to failure as previously described.[7,25,26] Before failure testing, the joint capsule, menisci, collateral ligaments, and posterior cruciate ligament were dissected from the joint, leaving the femur–ACL scar mass–tibia complex intact. The scar mass was bluntly inspected for presence and integrity of any suture material. For failure testing, the knee flexion angle was initially set at 30°. The tibia was mounted to the base of the MTS via a sliding X-Y platform with the femur unconstrained to rotation. Before initiating the tensile test, the femur was lowered until the load across the joint surface was +5 N of compression. A ramp at 20 mm/min was performed and the load-displacement data were recorded at 100 Hz. The yield load, failure load, linear stiffness, yield displacement, and failure displacement were calculated from the MTS load-displacement tracing. Biomechanical testing was done by an individual blinded to the surgical condition.

Micro-CT

Knees were scanned in a MicroCAT II (Siemens, Malvern, PA) micro-CT scanner at a resolution of 50 μm with a slice thickness of 0.09 mm to assess tunnel integrity. The scanner was set at 300 ms exposure, 72 kVp, and 500 μA in 1° increments for 360°. Each scan took approximately 10 minutes. Scans were aligned such that the bone tunnel was along the vertical axis using the free medical imaging software AMIDE (Andreas Loening, www.amide.sourceforge.net).

Size and density of the suture tunnels were each obtained in triplicate at 6 anatomical locations (proximal tunnel opening, proximal third of tunnel, proximal growth plate, distal growth plate, distal proximal third of tunnel, and distal tunnel opening) using circular or elliptical regions of interest at a right angle to the tunnel axis. Bone mineral density (BMD) was calculated as milligrams of hydroxyapatite per cubic centimeter. A phantom containing samples of known density was also scanned using the same protocol as the bone specimens, and density was measured in Amide and a plot of Amide units versus real units was created to provide BMD. BMD was also determined in normal bone surrounding each tunnel section. Additionally, the widest surface area of the affected growth plate and the growth plate density were measured. Because the same surgical methods and instruments (especially drill sizes) were used in both groups, tunnel diameters and density were assumed to be identical between the 2 groups at time zero.

Histologic Assessment

After micro-CT scanning, the tibia was retrieved and fixed in neutral buffered formalin for 1 week, decalcified in HCl, sectioned along the bone tunnel, dehydrated, and embedded in paraffin. Seven-micron sections were cut, placed onto pretreated glass slides, and stored at 48°C. Sections from each animal were stained with H&E. The affected growth plate was assessed for cellularity and suture residuals. Briefly, the number of cells within three 0.1-mm^2 areas was measured by 2 independent, blinded reviewers and the results were averaged. At each location, the total number of cells were counted and divided by the area of analysis to yield the cell density (n/mm^2).

Statistical Analysis

The sample size of this study was based on an a priori power calculation. A difference of 20% between groups was deemed clinically significant. Using biomechanical data from

earlier studies,[6,7,26,31] we therefore wanted to test for a minimum difference of displacement, load, and stiffness between ACL repair with 2 different suture types of 20% with an α (*P* value) of 5% and a minimum power of 95%. The standard deviations in prior studies were 8.2% for displacement, 9.1% for load, and 9.5% for stiffness. Assuming similar SDs for this study, a difference of 20% between groups would result in effect sizes for each of 2.5, 2.2, and 2.1, respectively. Thus, to achieve 95% power at minimum effect size of 2, our required sample size was 8 animals per group, or 16 animals in total.

Micro-CT outcomes were compared across groups using 2-tailed *t* tests. Analyses were done for averages for the whole tunnel and for the growth plate individually. All biomechanical outcomes for tensile testing were normalized for intact ACL values to account for potential interanimal differences. Results were therefore used as relative values (experimental/intact) and are given in "percent of intact ACL." For laxity testing side-to-side differences (experimental minus intact) in millimeters are given. All biomechanical outcomes were tested in generalized mixed models, a modeling method that allows using both within-animal comparisons (normal *v* contralateral knees) and across-animal comparisons (ACL reconstruction *v* repair *v* trans-section) in the same statistical test. Model fit was assessed by examination of the model residuals.

All calculations were done using SAS (SAS, Cary, NC). An α of 5% was considered significant, and Holm adjustment was used to adjust *P* values for multiple testing. Results are given as mean with 95% confidence intervals (CIs).[32]

Results

Animal Welfare

All animals recovered well from surgery. Full weight-bearing status was achieved within 48 to 72 hours for all groups. All animals reached the 15-week time point without infections or other significant postoperative complications. No residual suture material was found in any of the knees in the absorbable suture repair group during macroscopic assessment prior to tensile testing. All nonabsorbable sutures had ruptured by the 15-week time point, with ruptures occurring in the distal half of the intra-articular portion.

Physical Examination

Range of motion for the treated knees was adjusted for the values for intact knees and compared across groups. There were no differences in flexion ($P = .442$), extension ($P = .999$), or thigh circumference ($P = .337$) preoperatively. Table 1 shows the values for flexion, extension, and thigh circumference for both groups preoperatively and at the time of harvest. The changes from preoperatively to harvest in the 3 end points were not different across groups (Table 1).

Micro-CT: Entire Suture Tunnel

At 15 weeks postoperatively, there was a significant difference in average tibial tunnel diameter between absorbable and nonabsorbable sutures ($P < .001$), with significantly larger diameters in the nonabsorbable suture group of 4.4 mm (95% CI, 4.1 to 4.7) compared with 1.8 mm (95% CI, 1.6 to 1.9) in the absorbable suture group. There was also a significant difference in the average tunnel area ($P < .001$), with 15.2 mm^2 (95% CI, 12.7 to 17.6) for nonabsorbable sutures and 2.7 mm^2 (95% CI, 2.1 to 3.2) for absorbable sutures.

However, there was no significant difference in tunnel density between the 2 groups ($P = .355$) with 1,053.0 mg/cm^3 (95% CI, 1,046.2 to 1,059.7) for nonabsorbable and 1,068.1 mg/cm^3 (95% CI, 1,051.5 to 1,084.7) for absorbable sutures. The average mineral density of the

surrounding healthy bone was 1,133.9 mg/cm^3 (95% CI, 1,119.1 to 1,148.6), which was significantly higher than the tunnel density in both groups ($P < .001$ for both) (Fig 1).

Micro-CT: Growth Plate

A significantly greater area and volume of the growth plate were affected in the nonabsorbable group compared with the absorbable group at 15 weeks of follow-up (both $P < .001$). The average area of affected growth plate was 21.8 mm^2 (95% CI, 17.5 to 26) versus 6.5 mm^2 (95% CI, 4.7 to 8.2) with nonabsorbable and absorbable sutures. The affected volumes were 46.3 cm^3 (95% CI, 38.3 to 54.3) versus 5.3 cm^3 (95% CI, 3.4 to 7.1).

Significant differences in growth plate tunnel density were seen between the 2 groups, with the higher density seen in the group treated with absorbable sutures ($P = .020$). The average tunnel density at the proximal and distal physis was 1,080.9 mg/cm^3 (95% CI, 1,051.4 to 1,110.3) for absorbable sutures but lower at 1,045.5 mg/cm^3 (95% CI, 1,040.4 to 1,050.5) in the nonabsorbable group. Again, the mineral density of the growth plate was significantly lower than that of surrounding healthy bone tissue in both groups ($P < .001$ for both). All animals in the nonabsorbable suture group showed bone spicules crossing the physis, whereas such spicules were seen in only 50% of animals treated with absorbable sutures ($P = .021$) (Fig 2).

Anteroposterior Laxity at 15 Weeks

There was no significant difference in AP laxity between groups when measured at 30° ($P = .5117$), 60° ($P = .3150$), and 90° ($P = .4297$) of knee flexion. The average differences in AP laxity between treated and intact knees at 30° of flexion were 6.1 mm (95% CI, 3.3 to 8.9) for the absorbable group and 4.8 mm (95% CI, 2.6 to 7.1) for the nonabsorbable group. The corresponding values at 60° were 10.7 mm (95% CI, 9.1 to 12.3) versus 9.9 mm (95% CI, 8.3 to 11.4) and at 90° of flexion 8.1 mm (95% CI, 7.2 to 8.9) versus 6.8 mm (95% CI, 5.8 to 7.8), respectively (Fig 3).

Tensile Testing at Time Zero

At time zero, there was no statistically significant difference for yield displacement ($P = .122$), but there was a significant difference for failure displacement ($P = .003$) between the 2 groups. The average yield and failure displacements of the repairs for the absorbable suture group were 5.68 mm (95% CI, 4.5 to 6.9) and 25.17 mm (95% CI, 22.94 to 27.41), respectively. This corresponds to 82% and 316% of the values of displacements for an intact ACL. The displacements for the repairs of the nonabsorbable group were 11.21 mm (95% CI, 5.3 to 17.1) and 33.7 mm (95% CI, 30.9 to 36.5), which corresponded to 162% and 423% of intact values, respectively.

The yield load and failure load were both higher in the nonabsorbable suture group than in the absorbable suture group ($P = .037$ for yield and $P < .001$ for failure). The mean loads for the repairs of the absorbable suture group were 86.8 N (95% CI, 73.7 to 100.0) to yield and 334.6 N (95% CI, 302.4 to 366.7) to failure. Loads for the nonabsorbable suture group were 158.4 N (95% CI, 107.5 to 209.26) to yield and 477.1 N (95% CI, 456.2 to 498.1) to failure. Absorbable sutures reached 12% and 42% of intact values for yield and failure load; nonabsorbable sutures reached 21% and 59%.

There was no statistically significant difference in the linear stiffness between the groups ($P = .340$). The linear stiffness of the repair tissue for the absorbable group was 21.6 N/mm (95% CI, 20.5 to 22.7) and for the nonabsorbable group 25.5 N/mm (95% CI, 18.3 to 32.7), corresponding to 14% and 17% of normal, porcine ACL values.

Tensile Testing at 15 Weeks

There was no statistically significant difference for yield displacement ($P = .473$), but there was a borderline significant difference for failure displacement ($P = .057$) when the 2 groups were compared. The average yield and failure displacements of the repairs for the absorbable suture group were 7.1 mm (95% CI, 4.6 to 9.6) and 8.0 mm (95% CI, 5.5 to 10.6), respectively. This corresponds to 76% ± 13% and 65% ± 25% of the values of displacements for the intact, contralateral knee. The displacements for the repairs of the nonabsorbable group were 5.8 mm (95% CI, 4.6 to 6.8) and 6.7 mm (95% CI, 4.9 to 8.5), which corresponded to 84% ± 24% and 81% ± 20% of the intact knee values, respectively (Fig 4).

The yield load and failure load were both higher in the nonabsorbable suture group than in the absorbable suture group ($P = .014$ for yield and $P = .002$ for failure). The mean loads for the repairs of the absorbable suture group were 156.5 N (95% CI, 92.0 to 221.0) to yield and 173.0 N (95% CI, 102.7 to 243.2) to failure. In comparison, loads for the nonabsorbable suture group were 194.1 N (95% CI, 104.5 to 283.6) to yield and 211 N (95% CI, 120.9 to 301.0) to failure. Bio-enhanced repair with absorbable sutures reached 16.8% ± 11% and 16.9% ± 10% of intact values for yield and failure load, whereas repairs with nonabsorbable sutures reached 22.8% ± 11% and 23.3% ± 11% of intact (Fig 5). The mean load to failure for the intact porcine ACLs was 996.5 ± 149.1 N.

There was no statistically significant difference in the linear stiffness of the repairs between the 2 groups ($P = .531$). The linear stiffness of the repair tissue was 29.0 N/mm (95% CI, 18.7 to 39.3) for the absorbable group and 43.3 N/mm (95% CI, 22.4 to 64.3) for the nonabsorbable group. These values corresponded to 19% ± 10% and 25% ± 16% of the contralateral intact ACL.

Histologic Assessment

The histologic specimens showed sutures in the bone tunnels in all samples of the nonabsorbable group, but no suture residuals in the absorbable group. The formation of fibrovascular tissue between the suture strands was observed in only 2 specimens from the nonabsorbable group, compared with all but one absorbable specimen. However, in those areas with tissue formation, there was no statistically significant difference ($P = .300$) in cell counts between absorbable (640 ± 160 cells/mm^2) and nonabsorbable (370 ± 300 cells/mm^2) specimens. The physeal defects in line with the tunnels for the absorbable sutures were also filled with fibrovascular tissue with no chondrocytes noted. However, the physes for both groups did have an irregularity in shape at the site of the tunnel crossing with the physeal tunnel edges moving away from the joint in both femur and tibia (Fig 6).

Discussion

The purpose of this study was to test for differences in physeal structure and biomechanical outcomes after bioenhanced ACL repair using absorbable or nonabsorbable sutures. First, we found evidence for more growth plate disruption in the nonabsorbable suture group (Ethibond), which had larger tunnels, and lower BMD within the tunnels at the 15-week time point compared with the absorbable group (Vicryl). We also found that the use of nonabsorbable suture material produced significantly improved outcomes in structural properties in regard to the yield and failure loads and a trend for a lower failure displacement than the use of absorbable sutures. The fact that all sutures were disrupted at the time of biomechanical testing rules out that these differences in testing are attributable to the suture material itself but rather supports the assumption of an underlying difference in biologic response. However, the ruptured sutures might very well have influenced the

amount of stress shielding that had occurred, but we cannot say how great this effect may have been as it is unknown at what time point the sutures broke.

Work by prior investigators for physeal injury after surgical interventions has shown that the most persistent physeal injuries occur when a foreign material is placed across the physis. Factors associated with increased risk of physeal malfunction in prior animal studies have included posterior tunnel placement,[33,34] a high ratio of tunnel diameter to physeal surface area,[35–37] excessive graft tensioning,[38] incomplete tunnel filling by the graft,[39,40] and graft fixation across the physis.[41] In human patients, the vast majority of growth disturbances and angular deformities have been associated with graft fixation devices or bone-plugs leading to bony bars across the lateral distal femoral physis (54% of angular deformities) or epiphysiodetic effects of fixation devices crossing the tibial physis (27% of angular deformities).[42] In this study, with our relatively small ratio of tunnel diameter to physeal surface area, lack of excessive tensioning, and avoidance of fixation devices across the physes, we did not see any physeal disturbances, as in accordance with prior animal and clinical studies. In contrast, the incomplete tunnel filling seen in both suture groups did not appear to have a significant effect on premature physeal closure in this study.

We found significant differences in yield (157 ± 93 N for absorbable *v* 194 ± 120 N for nonabsorbable) and failure loads (173 ± 101 *v* 211 ± 122 N), in favor of nonabsorbable sutures at both time zero and 15 weeks. However, over time the gap between the 2 groups widened. We hypothesize that the nonabsorbable sutures offered more mechanical protection than absorbable sutures after the ACL repair and thus resulted in a better biomechanical outcome. This hypothesis is supported by clinical studies of suture repair of tibial eminence fractures, where excellent results have been shown with various types of nonabsorbable sutures, even over pin-and-screw fixation.

Micro-CT revealed larger and wider tunnels in the nonabsorbable suture group. Although the difference in tunnel density between the 2 groups was statistically significant, it was less than 5% and thus not likely to be of clinical significance. However, a closer look at the cartilaginous growth plate showed not only larger affected areas in the nonabsorbable group but also a significantly lower mineral density in the nonabsorbable suture group and a higher tendency for bony spur formation in the nonabsorbable suture group. Similar bony bridges were found in a recent study of the effects of transphyseal ACL reconstruction in skeletally immature sheep but were not associated with growth disturbances.[39] A recent article in the *Journal of Orthopedic Research* offers an explanation of this dissociation of bone bridges and physeal arrest by showing that these bony bridges are not so much a precocious ossification of the growth plate but rather dislodged osteoprogenitor cells from the bone marrow.[43] Although it is not unequivocally clear that these results will lead to a worse clinical outcome, they, at the very least, suggest a potentially greater injury to the growth plate.

The surgical technique as tested here in the porcine model is not yet in use clinically. However, as preclinical studies of bioenhanced ACL repair are showing promise,[14] it is possible that this technique will be in clinical practice in the next several years. Therefore, determining the effect of suture selection on physeal status and healing ligament strength was important prior to starting clinical studies of this technique. The porcine model was selected for this study because of the great similarities in wound healing, knee biomechanics, and hematology between the porcine and human species.

This study focused on bioenhanced ACL repair, but its findings are also meaningful for ACL eminence fractures. In such injuries, the ACL has typically avulsed with a piece of bone from the tibial spine. Displaced injuries are usually treated with suture fixation, or

screw fixation.[44–46] Gan et al.[47] and Tsukada et al.[48] found good results with tension wires and anterograde screw fixation. A study by Eggers et al.[49] compared sutures and screws and showed that suture fixation using nonabsorbable Ethibond has higher strength than screw fixation. However, until now there has been limited information on the effects of suture fixation on the physis.

Histologically, we found most of the tunnels in the nonabsorbable group filled with suture material and only little tissue in between the suture strands. This picture might change over time as tissue encompasses the sutures, but some remaining material will be present. In the absorbable group, we found no evidence of sutures and good tissue formation. The physes in the nonabsorbable groups were disrupted but the remaining sutures, whereas the absorbable group showed pivoting of the physis but no persistent defect. In those areas with sufficient space for new tissue to form, there was no difference in cell counts across the groups, suggesting no difference in the effect of the presence of the nonabsorbable sutures or the remnants of the absorbable sutures on cell growth.

Our study has potential shortcomings. We compared only 2 suture materials. These sutures were selected because they are commonly used in arthroscopic knee surgery. It cannot be ruled out with certainty that other sutures could respond differently. Nonetheless, there was a difference between the 2 suture types and hence further investigation is warranted. In addition, this study was performed in a large animal model where controlled rehabilitation is not an option. Whether a slower rehabilitation would result in a longer persistence of the intact nonabsorbable sutures, or even the absorbable sutures, and what effect that additional retention time would have require further study. Also, it should be noted that there was no "tunnel only" control group. However, prior studies, such as Shea et al.[50] in *Arthroscopy* or Meller et al.,[51] have already assessed the volumetric effect of transepiphyseal drilling. A recent systematic review published in *Arthroscopy* lists the risk factors for physeal growth disturbance after ACL reconstruction.[18] Finally, our model cannot fully reproduce the human situation. For example, we could not control postoperative rehabilitation in the animals. Likewise, the ACL injury was simulated with sharp transsection in the midsubstance. It is possible that a frayed disruption with associated cartilage and meniscal injury, as seen in the clinical situation, would heal differently. On the other hand, the frayed ends have a larger surface area, thus more contact, and might weave into each other, whereas the clean cuts may slide off. We followed these animals for 15 weeks, although clinical ACL studies usually follow patients for years. However, since we wanted to assess tunnel healing, 15 weeks has been found an appropriate time point to assess for permanent differences in tunnel healing, while at the same time being a reliable predictor of tissue healing in ACL repair.[5]

Conclusions

The use of absorbable sutures for ACL repair resulted in decreased physeal plate damage after 15 weeks of healing; however, use of nonabsorbable sutures resulted in 20% stronger repairs.

Acknowledgments

Supported by National Institutes of Health Grants R01-AR054099, R01-AR056834, and R01-AR052772.

The authors are indebted to Elise Magarian and Sophia L. Harrison for assistance during animal surgeries and to David Paller and Alison Biercevicz for assistance with mechanical testing. They are also grateful to Arthur Nedder, Kathryn Mullen, Kimberlie Hauser, and Mark Kelly for their veterinary expertise and care.

References

1. Murray MM. Current status and potential of primary ACL repair. Clin Sports Med. 2009; 28:51–61. [PubMed: 19064165]
2. Feagin JA Jr, Curl WW. Isolated tear of the anterior cruciate ligament: 5-Year follow-up study. Am J Sports Med. 1976; 4:95–100. [PubMed: 984289]
3. Murray MM, Spindler KP, Ballard P, Welch TP, Zurakowski D, Nanney LB. Enhanced histologic repair in a central wound in the anterior cruciate ligament with a collagen-platelet-rich plasma scaffold. J Orthop Res. 2007; 25:1007–1017. [PubMed: 17415785]
4. Mastrangelo AN, Haus BM, Vavken P, Palmer MP, Machan JT, Murray MM. Immature animals have higher cellular density in the healing anterior cruciate ligament than adolescent or adult animals. J Orthop Res. 2010; 28:1100–1106. [PubMed: 20127960]
5. Joshi SM, Mastrangelo AN, Magarian EM, Fleming BC, Murray MM. Collagen-platelet composite enhances biomechanical and histologic healing of the porcine anterior cruciate ligament. Am J Sports Med. 2009; 37:2401–2410. [PubMed: 19940313]
6. Murray MM, Palmer M, Abreu E, Spindler KP, Zurakowski D, Fleming BC. Platelet-rich plasma alone is not sufficient to enhance suture repair of the ACL in skeletally immature animals: An in vivo study. J Orthop Res. 2009; 27:639–645. [PubMed: 18991345]
7. Fleming BC, Magarian EM, Harrison SL, Paller DJ, Murray MM. Collagen scaffold supplementation does not improve the functional properties of the repaired anterior cruciate ligament. J Orthop Res. 2010; 28:703–709. [PubMed: 20058276]
8. Kroon ME, van Schie ML, van der Vecht B, van Hinsbergh VW, Koolwijk P. Collagen type 1 retards tube formation by human microvascular endothelial cells in a fibrin matrix. Angiogenesis. 2002; 5:257–265. [PubMed: 12911012]
9. Fufa D, Shealy B, Jacobson M, Kevy S, Murray MM. Activation of platelet-rich plasma using soluble type I collagen. J Oral Maxillofac Surg. 2008; 66:684–690. [PubMed: 18355591]
10. Harrison S, Vavken P, Kevy S, Jacobson M, Zurakowski D, Murray MM. Platelet activation by collagen provides sustained release of anabolic cytokines. Am J Sports Med. 2011; 39:729–734. [PubMed: 21398575]
11. Cheng M, Wang H, Yoshida R, Murray MM. Platelets and plasma proteins are both required to stimulate collagen gene expression by anterior cruciate ligament cells in three-dimensional culture. Tissue Eng Part A. 2010; 16:1479–1489. [PubMed: 19958169]
12. Vavken P, Fleming BC, Mastrangelo AN, Machan JT, Murray MM. Biomechanical outcomes after bioenhanced anterior cruciate ligament repair and anterior cruciate ligament reconstruction are equal in a porcine model. Arthroscopy. 2012; 28:672–680. [PubMed: 22261137]
13. Cheng M, Wang H, Yoshida R, Murray MM. Platelets and plasma proteins are both required to stimulate collagen gene expression by anterior cruciate ligament cells in three-dimensional culture. Tissue Eng Part A. 2010; 16:1479–1489. [PubMed: 19958169]
14. Harrison SL, Vavken P, Murray MM. Erythrocytes inhibit ligament fibroblast proliferation in a collagen scaffold. J Orthop Res. 2011; 29:1361–1366. [PubMed: 21445984]
15. Vavken P, Murray MM. Translational studies in anterior cruciate ligament repair. Tissue Eng Part B Rev. 2010; 16:5–11. [PubMed: 20143926]
16. Mastrangelo AN, Haus BM, Vavken P, Palmer MP, Machan JT, Murray MM. Immature animals have higher cellular density in the healing anterior cruciate ligament than adolescent or adult animals. J Orthop Res. 2010; 28:1100–1106. [PubMed: 20127960]
17. Mastrangelo AN, Magarian EM, Palmer MP, Vavken P, Murray MM. The effect of skeletal maturity on the regenerative function of intrinsic ACL cells. J Orthop Res. 2010; 28:644–651. [PubMed: 19890988]
18. Vavken P, Murray M. Treating anterior cruciate ligament tears in skeletally immature patients. Arthroscopy. 2011; 27:704–716. [PubMed: 21552340]
19. Uchida A, Tohyama H, Nagashima K, et al. Stress deprivation simultaneously induces over-expression of interleukin-1 beta, tumor necrosis factor-alpha, and transforming growth factor-beta in fibroblasts and mechanical deterioration of the tissue in the patellar tendon. J Biomech. 2005; 38:791–798. [PubMed: 15713300]

20. Majima T, Yasuda K, Tsuchida T, et al. Stress shielding of patellar tendon: Effect on small-diameter collagen fibrils in a rabbit model. J Orthop Sci. 2003; 8:836–841. [PubMed: 14648274]
21. Agrawal CM, Athanasiou KA. Technique to control pH in vicinity of biodegrading PLA-PGA implants. J Biomed Mater Res. 1997; 38:105–114. [PubMed: 9178737]
22. An YH, Woolf SK, Friedman RJ. Pre-clinical in vivo evaluation of orthopaedic bioabsorbable devices. Biomaterials. 2000; 21:2635–2652. [PubMed: 11071614]
23. Athanasiou KA, Agrawal CM, Barber FA, Burkhart SS. Orthopaedic applications for PLA-PGA biodegradable polymers. Arthroscopy. 1998; 14:726–737. [PubMed: 9788368]
24. Athanasiou KA, Niederauer GG, Agrawal CM. Sterilization, toxicity, biocompatibility and clinical applications of polylactic acid/polyglycolic acid copolymers. Biomaterials. 1996; 17:93–102. [PubMed: 8624401]
25. Murray MM, Magarian E, Zurakowski D, Fleming BC. Bone-to-bone fixation enhances functional healing of the porcine anterior cruciate ligament using a collagen-platelet composite. Arthroscopy. 2010; 26(suppl):S49–S57. [PubMed: 20810092]
26. Murray MM, Magarian EM, Harrison SL, Mastrangelo AN, Zurakowski D, Fleming BC. The effect of skeletal maturity on functional healing of the anterior cruciate ligament. J Bone Joint Surg Am. 2010; 92:2039–2049. [PubMed: 20810854]
27. Sanz LE, Patterson JA, Kamath R, Willett G, Ahmed SW, Butterfield AB. Comparison of Maxon suture with Vicryl, chromic catgut, and PDS sutures in fascial closure in rats. Obstet Gynecol. 1988; 71:418–422. [PubMed: 3126470]
28. Storch M, Scalzo H, Van Lue S, Jacinto G. Physical and functional comparison of Coated VICRYL Plus Antibacterial Suture (coated polyglactin 910 suture with triclosan) with Coated VICRYL Suture (coated polyglactin 910 suture). Surg Infect (Larchmt). 2002; 3(suppl 1):S65–S77. [PubMed: 12573041]
29. Najibi S, Banglmeier R, Matta J, Tannast M. Material properties of common suture materials in orthopaedic surgery. Iowa Orthop J. 2010; 30:84–88. [PubMed: 21045977]
30. Fleming BC, Carey JL, Spindler KP, Murray MM. Can suture repair of ACL transection restore normal anteroposterior laxity of the knee? An ex vivo study. J Orthop Res. 2008; 26:1500–1505. [PubMed: 18528857]
31. Fleming BC, Spindler KP, Palmer MP, Magarian EM, Murray MM. Collagen-platelet composites improve the biomechanical properties of healing anterior cruciate ligament grafts in a porcine model. Am J Sports Med. 2009; 37:1554–1563. [PubMed: 19336614]
32. Vavken P, Heinrich KM, Koppelhuber C, Rois S, Dorotka R. The use of confidence intervals in reporting orthopaedic research findings. Clin Orthop Relat Res. 2009; 467:3334–3339. [PubMed: 19333667]
33. Shea KG, Apel PJ, Pfeiffer RP. Anterior cruciate ligament injury in paediatric and adolescent patients: A review of basic science and clinical research. Sports Med. 2003; 33:455–471. [PubMed: 12744718]
34. Shea KG, Apel PJ, Pfeiffer RP, Traughber PD. The anatomy of the proximal tibia in pediatric and adolescent patients: Implications for ACL reconstruction and prevention of physeal arrest. Knee Surg Sports Traumatol Arthrosc. 2007; 15:320–327. [PubMed: 16909299]
35. Guzzanti V, Falciglia F, Stanitski C. Physeal-sparing intraarticular anterior cruciate ligament reconstruction in preadolescents. Am J Sports Med. 2003; 31:949–953. [PubMed: 14623662]
36. Guzzanti V, Falciglia F, Stanitski C. Preoperative evaluation and anterior cruciate ligament reconstruction technique for skeletally immature patients in Tanner stages 2 and 3. Am J Sports Med. 2003; 31:941–948. [PubMed: 14623661]
37. Houle JB, Letts M, Yang J. Effects of a tensioned tendon graft in a bone tunnel across the rabbit physis. Clin Orthop Relat Res. 2001; (391):275–281. [PubMed: 11603681]
38. Edwards TB, Greene CC, Baratta RV, Zieske A, Willis RB. The effect of placing a tensioned graft across open growth plates. A gross and histologic analysis. J Bone Joint Surg Am. 2001; 83:725–734. [PubMed: 11379743]
39. Seil R, Pape D, Kohn D. The risk of growth changes during transphyseal drilling in sheep with open physes. Arthroscopy. 2008; 24:824–833. [PubMed: 18589272]

40. Stadelmaier DM, Arnoczky SP, Dodds J, Ross H. The effect of drilling and soft tissue grafting across open growth plates. A histologic study. Am J Sports Med. 1995; 23:431–435. [PubMed: 7573652]
41. Chudik S, Beasley L, Potter H, Wickiewicz T, Warren R, Rodeo S. The influence of femoral technique for graft placement on anterior cruciate ligament reconstruction using a skeletally immature canine model with a rapidly growing physis. Arthroscopy. 2007; 23:1309–1319. [PubMed: 18063175]
42. Kocher M, Saxon H, Hovis W, Hawkins R. Management and complications of anterior cruciate ligament injuries in skeletally immature patients: Survey of the Herodicus Society and The ACL Study Group. J Pediatr Orthop. 2002; 22:452–457. [PubMed: 12131440]
43. Xian CJ, Zhou FH, McCarty RC, Foster BK. Intra-membranous ossification mechanism for bone bridge formation at the growth plate cartilage injury site. J Orthop Res. 2004; 22:417–426. [PubMed: 15013105]
44. Hapa O, Barber FA, Suner G, et al. Biomechanical comparison of tibial eminence fracture fixation with high-strength suture, EndoButton, and suture anchor. Arthroscopy. 2012; 28:681–687. [PubMed: 22284410]
45. Lubowitz JH, Elson WS, Guttmann D. Part I: Arthroscopic management of tibial plateau fractures. Arthroscopy. 2004; 20:1063–1070. [PubMed: 15592236]
46. Lubowitz JH, Elson WS, Guttmann D. Part II: Arthroscopic treatment of tibial plateau fractures: Intercondylar eminence avulsion fractures. Arthroscopy. 2005; 21:86–92. [PubMed: 15650672]
47. Gan Y, Xu D, Ding J, Xu Y. Tension band wire fixation for anterior cruciate ligament avulsion fracture: Biomechanical comparison of four fixation techniques. Knee Surg Sports Traumatol Arthrosc. 2012; 20:909–915. [PubMed: 21863305]
48. Tsukada H, Ishibashi Y, Tsuda E, Hiraga Y, Toh S. A biomechanical comparison of repair techniques for anterior cruciate ligament tibial avulsion fracture under cyclic loading. Arthroscopy. 2005; 21:1197–1201. [PubMed: 16226647]
49. Eggers AK, Becker C, Weimann A, et al. Biomechanical evaluation of different fixation methods for tibial eminence fractures. Am J Sports Med. 2007; 35:404–410. [PubMed: 17170161]
50. Shea KG, Belzer J, Apel PJ, Nilsson K, Grimm NL, Pfeiffer RP. Volumetric injury of the physis during single-bundle anterior cruciate ligament reconstruction in children: A 3-dimensional study using magnetic resonance imaging. Arthroscopy. 2009; 25:1415–1422. [PubMed: 19962068]
51. Meller R, Willbold E, Hesse E, et al. Histologic and biomechanical analysis of anterior cruciate ligament graft to bone healing in skeletally immature sheep. Arthroscopy. 2008; 24:1221–1231. [PubMed: 18971051]

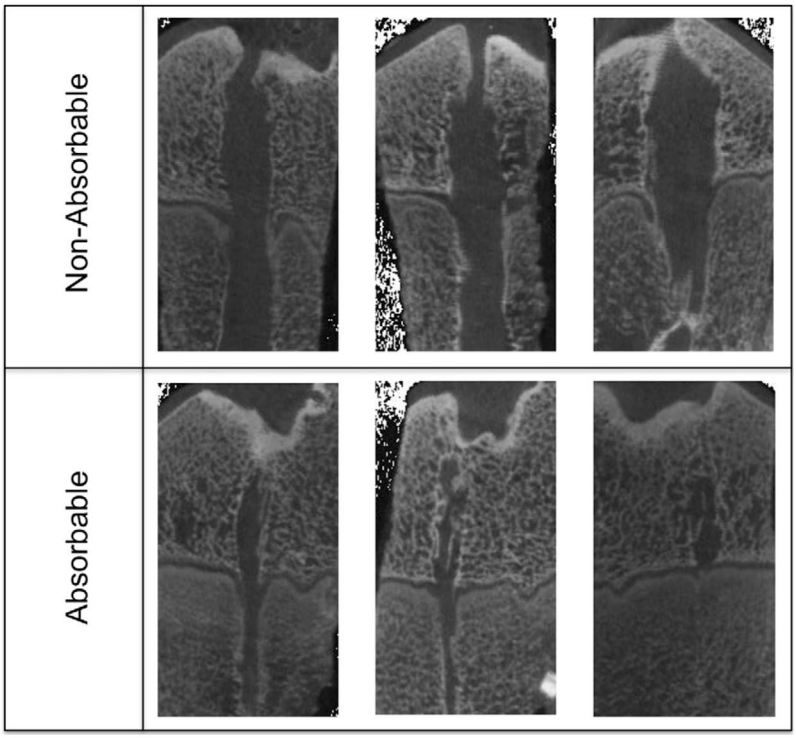

Fig 1.
Panel of micro-CT scans. The top row shows nonabsorbable group versus absorbable group at the bottom at the same magnification. The larger physeal damage in the nonabsorbable group is striking. Also, bone spurs across the physes can be seen in both rows.

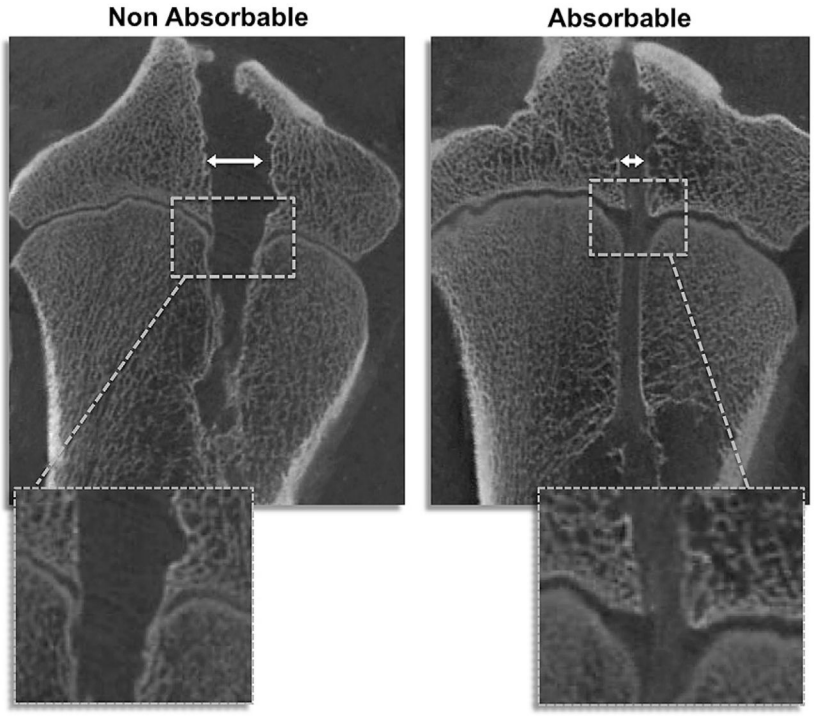

Fig 2.

Representative micro-CT images. Note the wider bone tunnel (with arrows) in the nonabsorbable sample. Also, the affected growth plate area is significantly larger in the nonabsorbable suture groups, and bony bars can be seen in the magnification (white squares).

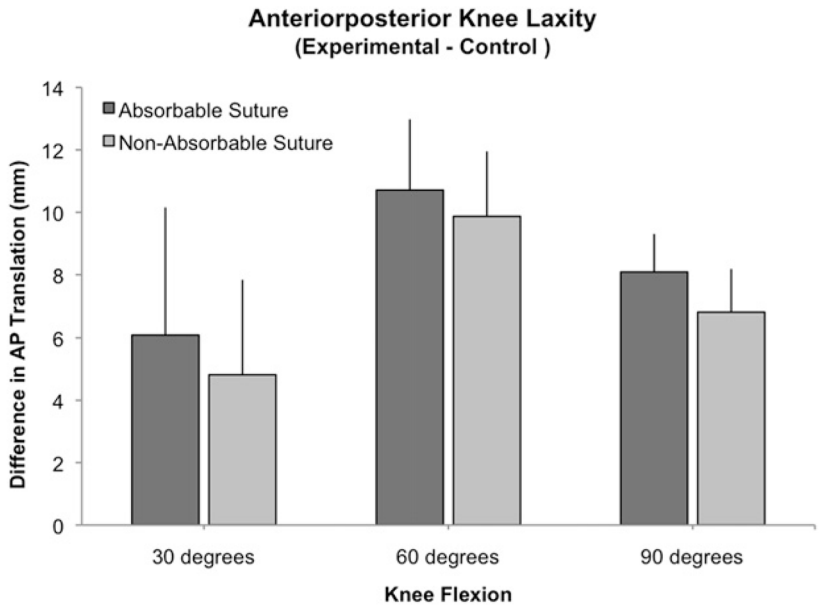

Fig 3.

Outcomes for anteroposterior knee laxity for the experimental knees adjusted for intact ACL (with SD). Contrary to tensile testing this adjustment is not the percentage of intact, but the difference of experimental and intact knees.

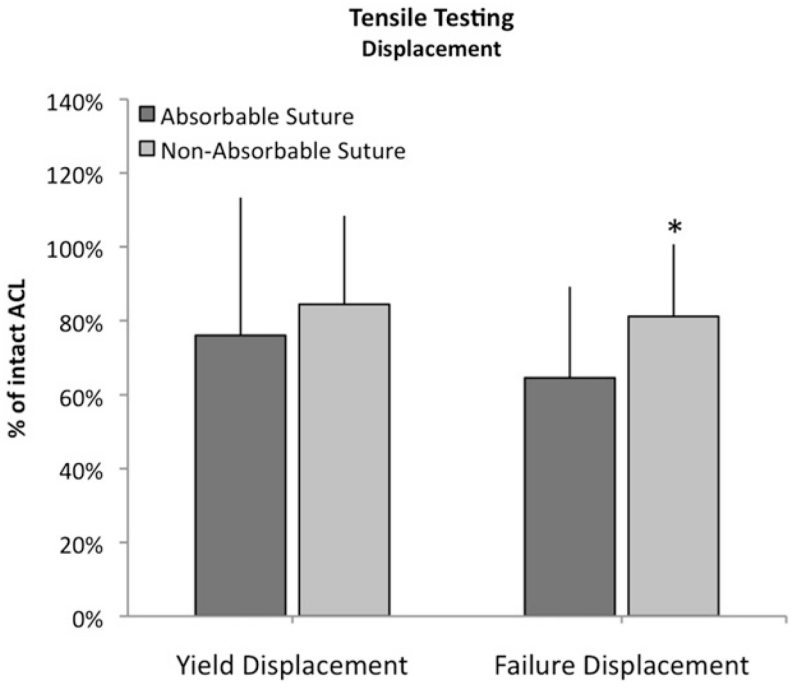

Fig 4.
Outcomes for displacement for the experimental knees adjusted for intact ACL (with SD) at 15 weeks. *P = .0572.

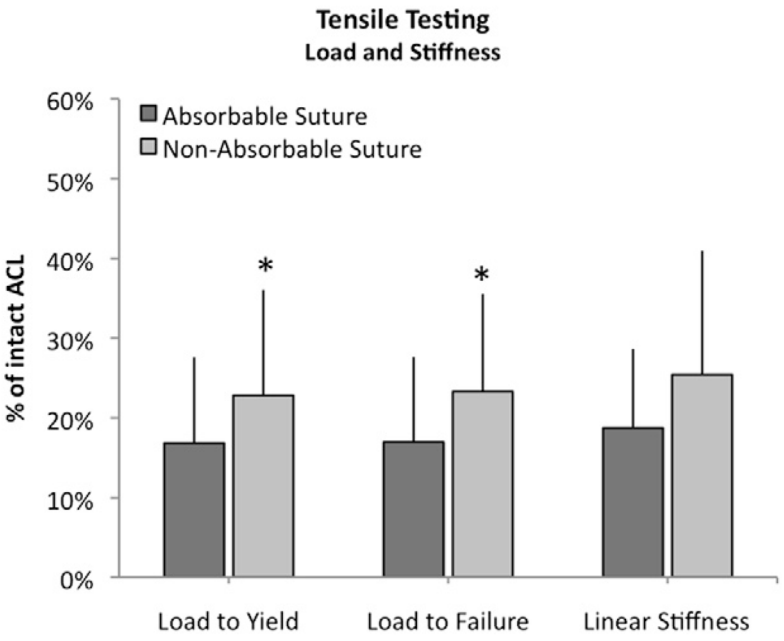

Fig 5.

Outcomes for load and stiffness for the experimental knees adjusted for intact ACL (with SD) at 15 weeks. *$P \leq .05$.

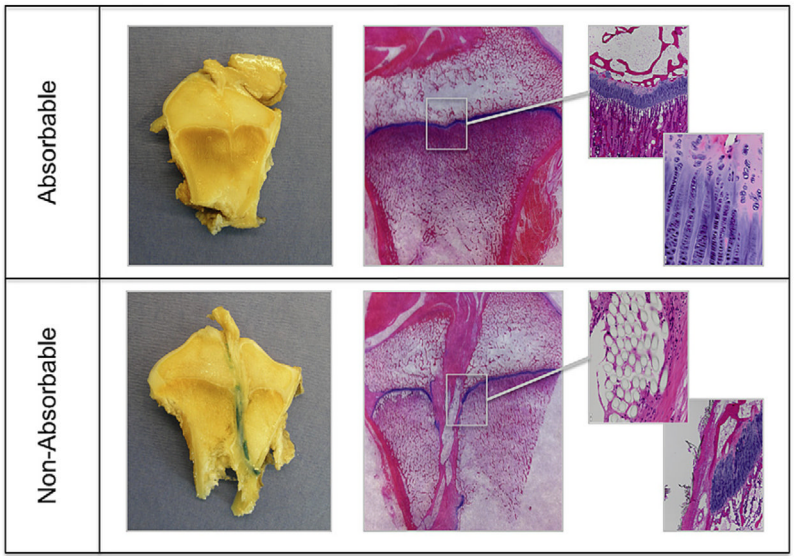

Fig 6.

Macroscopic and histologic pictures. The top row shows nonabsorbable group versus absorbable group at the bottom at the same magnification. In the absorbable group, no suture material is visible and the physis has healed completely with slight dimpling, but largely normal tissue. In the nonabsorbable group, the sutures are still present and can be seen in the histologic section, as they disrupt the physis.

Table 1

Physical Exam: Experimental Knees

	Absorbable	Nonabsorbable	*P Value*[*]
Flexion (°)			
Preoperative	141.9 ± 5.9	142.9 ± 4.9	
Harvest	145.0 ± 5.0	140.0 ± 5.8	
Difference	3.6 ± 12.1	−2.9 ± 4.9	.218
Extension (°)			
Preoperative	34.4 ± 5.0	34.3 ± 9.3	
Harvest	32.9 ± 3.9	42.9 ± 7.6	
Difference	3−.1 ± 4.9	4.3 ± 9.3	.132
Thigh circumference (cm)			
Preoperative	23.5 ± 0.5	21.1 ± 1.1	
Harvest	27.9 ± 1.2	25.7 ± 0.8	
Difference	4.4 ± 1.3	4.6 ± 1.1	.828

[*] For the comparison of difference over time across groups, without adjustment.